

## Evidence for density-wave domain structure in a mixed-band low-dimensional organic conductor

G. J. Athas, J. S. Brooks, and S. Valfells

*Department of Physics, Boston University, Boston, Massachusetts 02215*

S. J. Klepper

*Francis Bitter National Magnet Laboratory, Massachusetts Institute of Technology, Cambridge, Massachusetts 02139*

M. Tokumoto, N. Kinoshita, T. Kinoshita, and Y. Tanaka

*Electrotechnical Laboratory, Tsukuba, Ibaraki 305, Japan*

(Received 15 July 1994; revised manuscript received 6 October 1994)

We have used angular-dependent magnetoresistance to probe the anomalous low-temperature state in the two-band (quasi-one- and -two-dimensional) organic conductor family  $\alpha$ -(BEDT-TTF)<sub>2</sub>MHg(SCN)<sub>4</sub>, where BEDT-TTF stands for bis(ethylenedithio)tetrathiafulvalene. Our results provide strong evidence for a mixed state of both normal-metallic and Peierls-like domains with correspondingly different electronic structure. The different attributes of these coexisting domains are shown to be responsible for the complex magnetotransport phenomena in these materials, including the strong hysteretic behavior and the quantum-oscillation wave forms.

In this paper we propose that the low-temperature state of a well-studied organic-conductor family consists of a configuration of metallic and density-wave domains. The layered organic conductors  $\alpha$ -(BEDT-TTF)<sub>2</sub>MHg(SCN)<sub>4</sub> ( $M=K, Rb, Tl, \text{ or } NH_4$ ), where BEDT-TTF stands for bis(ethylenedithio)tetrathiafulvalene, have a combination of both quasi-one-dimensional and quasi-two-dimensional (Q1D and Q2D) Fermi surfaces<sup>1</sup> (FS's) as shown in Fig. 1. The members of this isostructural family can be classified by their low-temperature ground states;  $M=NH_4$  becomes a superconductor at 1 K, while below  $T_{DW}=8-10$  K (where DW denotes density wave),  $M=K, Rb,$  and  $Tl$  enter a low-temperature state (LTS) characterized by unusual magnetotransport effects (see below). This LTS is thought to be the result of a Peierls instability in the Q1D band, which induces either a spin or charge<sup>2-4</sup> DW below the characteristic temperature  $T_{DW}$ .

The coexistence of the Q2D FS (which remains metallic below  $T_{DW}$ ) masks the onset of insulating behavior in the Q1D FS, and hence only a small rise in the resistivity at  $T_{DW}$  is observed in an otherwise decreasing resistivity with lower temperatures. The new periodicity introduced by the density-wave nesting vector does, however, cause the Q2D FS to reconstruct<sup>5</sup> along the lines shown in Fig. 1. Associated with the LTS are several distinct features in magnetotransport (see Figs. 1-4).

(1) There is a giant magnetoresistance that peaks at about 10 T ( $H_{max}$ ), followed by a precipitous drop at the so-called "kink field"  $H_k$  in the range 20-30 T.<sup>6</sup>

(2) There is strong hysteretic behavior in the magnetoresistance for magnetic-field sweeps in and out of the kink-field region.<sup>7</sup>

(3) Dual-peak Shubnikov-de Haas (SdH) oscillations (resulting in anomalously large second-harmonic content in the Fourier transform) associated with the fundamental hole-band closed-orbit frequency ( $\alpha=670$  T for  $M=Tl$ ) are observed.<sup>8</sup> Also observed is a SdH frequency ( $\beta=4261$  T for

$M=Tl$ ) associated with 100% of the first Brillouin zone of the normal metallic Fermi surface.<sup>9</sup>

(4) Angular-dependent magnetoresistance oscillations (ADMRO's) (whose strong anisotropy and oscillatory behavior led to the notion of a reconstructed Fermi surface) are observed.<sup>10</sup>

In this paper we argue that the dual-peak SdH oscillations, hysteretic behavior, and observation of the magnetic-breakdown orbit ( $\beta$ ) that is, in principle, inconsistent with a reconstructed FS, must be manifestations of mixed-state behavior. In our model, metallic and density-wave domains coexist in the LTS, and each contributes to the magnetotransport phenomena. We use the different angular-dependent properties of these two states to identify their individual contributions to the LTS magnetoresistance. This work was performed at the Francis Bitter National Magnet Laboratory in Cambridge, Massachusetts and at the National High Magnetic Field Laboratory in Tallahassee, Florida.

We begin our discussion with the ADMRO phenomenon, as shown in Fig. 1. Here a sample is rotated along some axis in the  $a$ - $c$  (conducting) plane in a constant magnetic field. Oscillatory sharp minima are observed that are periodic in  $\tan\varphi$ , where  $\varphi$  is the angle between the  $b^*$  (least conducting) axis of the sample and the applied magnetic field. The angular location of the minima are independent of field and temperature, implying that these oscillations are due solely to the geometrical properties of the Fermi surface, and not the result of a phase transition. The observation that the minimum in the period of  $\tan\varphi$  occurs for an axis of rotation somewhere between 20° and 30° away from the  $k_c$  axis has led to the assertion<sup>5</sup> that the Q2D FS reconstructs at low temperature as shown in Fig. 1.

There is some variation with regards to the value of the proposed nesting vector  $Q$  in various reports (Refs. 5 and 11-14), but in our work for  $M=Tl$  and  $Rb$ , the value  $Q=(\pi/8a, 3\pi/8c, \pi/2b)$  is most consistent. We note that the resulting nesting configuration in the new, reconstructed Brillouin zone is shown in Fig. 1.

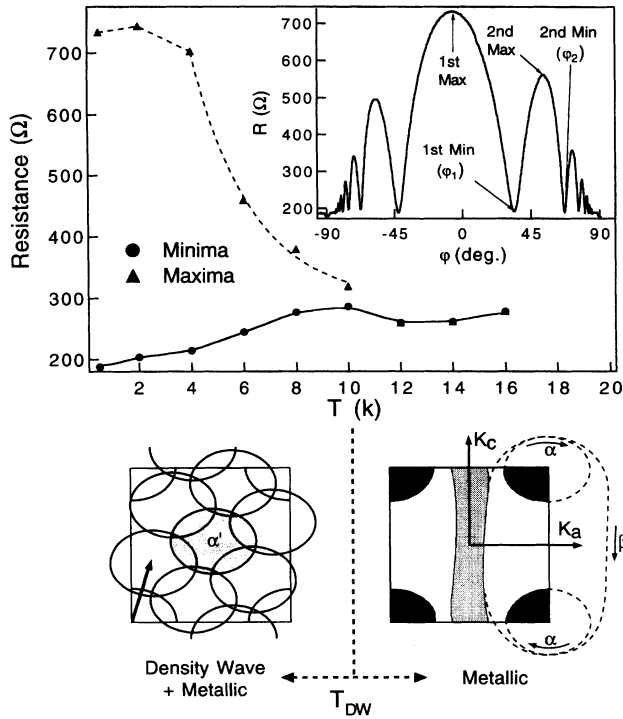


FIG. 1. Temperature dependence of the ADMRO extrema above and below the LTS phase transition ( $T_{DW}=10$  K) for  $M=Rb$  at  $H=14$  T. The inset shows ADMRO at  $T=0.5$  K with arrows indicating the extremal points relevant to this paper. Arrhenius analysis of the maximum between  $4 < T < 10$  results in a  $\Delta \approx 10$  K gap. The calculated metallic state FS, and the proposed coexistence of the metallic and reconstructed density-wave FS are shown separated by the LTS phase boundary. Magnetic-breakdown trajectories and the DW nesting vector  $Q$  (arrow) are highlighted.

loun zone (BZ) closely resembles that seen in magnesium.<sup>15</sup> This choice of  $Q$  provides a magnetic-breakdown network with no open orbits. All but the smallest of the closed orbits are the result of magnetic breakdown, with a probability  $P_{MB} = \exp(-H_0/H)$  where  $H_0 = mE_g^2/e\hbar E_f$  and  $E_g^2/E_f \sim \Delta k/k_f$ .<sup>16</sup> Here  $\Delta k$  is the momentum needed for a carrier to tunnel from one orbit to another. The probability increases with magnetic field. The giant magnetoresistance is the result of the many extended trajectories possible in this complex breakdown network.<sup>17</sup> For adjacent orbits with very small dispersion in the  $b^*$  direction (i.e., a nearly ideal two-dimensional FS),  $\Delta k$  is expected to increase with angle  $\varphi$  from purely geometrical considerations. Hence  $P_{MB}$ , and thereby the giant magnetoresistance, will decrease monotonically with  $\varphi$  as is the case with the ADMRO background in Fig. 1. What is unusual is that the giant magnetoresistance appears to nearly vanish at singular points,  $\varphi_n$  ( $n=0, \pm 1, \pm 2$ , etc.), with the period  $\tan\varphi$ . We suggest that at these special angles the magnetic-breakdown probability must approach zero. To punctuate this observation, we note the temperature dependence of the maxima and minima of the ADMRO signal. The maxima follow an activated-type behavior below  $T_{DW}$  that is characteristic of the evolution of a density-wave-type state,<sup>18</sup> but the minima follow a strictly metallic-type temperature dependence. We assert here that at

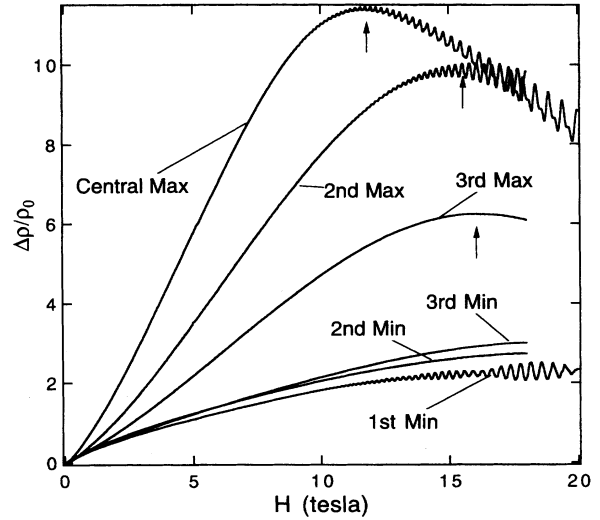


FIG. 2. Magnetoresistance of the first three ADMRO maxima and minima in  $M=Ti$  at 1.2 K. The arrows indicate the location of the MR turnover point  $H_{max}$  for the ADMRO maxima, which is characteristic of a magnetic-breakdown network. There is no observable  $H_{max}$  along the minima that become saturating. The SdH oscillations reduce in amplitude with increasing angle independent of the ADMRO, and dual-peak oscillations are faintly observable at the central maxima.

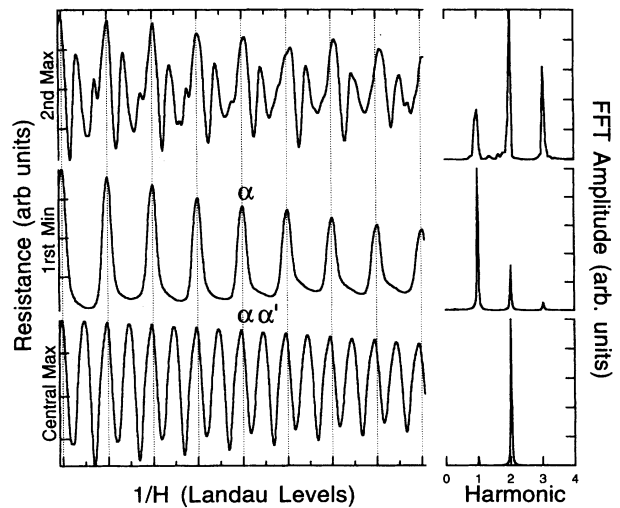


FIG. 3. SdH oscillations at 100 mK in  $M=Ti$  for the first two maxima and  $\varphi_n$ . The oscillations are plotted vs inverse magnetic field ( $1/H$ ), and are compensated for the  $1/\cos\varphi$  frequency dependence of the higher-angle sweeps. Disappearance of the second-series SdH component is observed along the first minima and emphasized in the fast-Fourier-transform results. The single-series oscillations at  $\varphi_n$  are sawtooth in shape, indicative of highly two-dimensional behavior. The reduced second-series oscillations at the second maximum indicate that they are more sensitive to angle than the first series, consistent with the proposed magnetic-breakdown model.

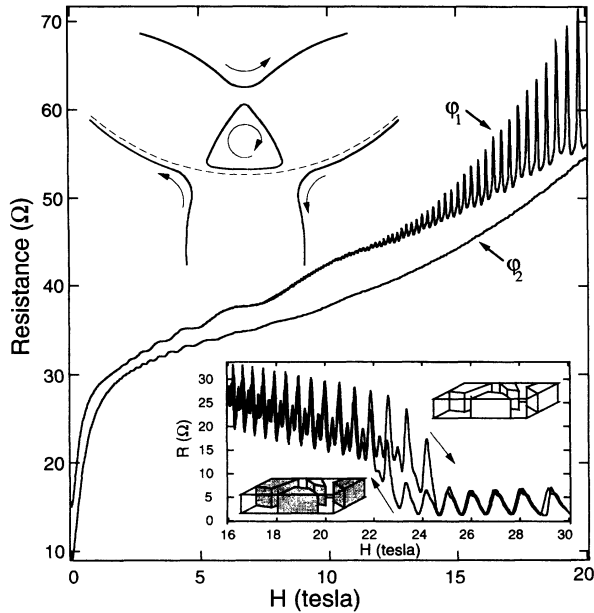


FIG. 4. Full field sweep of  $M=TI$  at 100 mK along  $\varphi_1$  and  $\varphi_2$ . Slow SdH oscillations appear at both these angles corresponding to a zero-angle area of  $\sim 10$  T (SdH oscillations corresponding to  $\alpha$  are suppressed at the large-angle  $\varphi_2$ ). The upper-left inset identifies the origin of this oscillation at the small triangular-hole orbit at the MB junctions. The solid lines represent Bragg-scattered paths, while the dashed line is the high-field magnetic-breakdown limit. The kink field hysteresis for  $M=K$  is shown in the lower-right inset. Below  $H_k$ , domains of reconstructed density-wave (shaded) and normal metallic (clear) regions coexist, while above the kink, all regions are normal metallic.

$\varphi_n$ , because the magnetic-breakdown probability (and hence the giant magnetoresistance) is removed, only the coexisting metallic behavior is observable.

The field dependence of the giant magnetoresistance is also strongly suppressed at  $\varphi_n$  as is shown in Fig. 2. Here we see that at the minima the magnetoresistance is sublinear, as opposed to superlinear at the maxima, and there is no turn-over point in the magnetoresistance corresponding to  $H_{\max}$ . The observation of  $H_{\max}$  is a consequence of shifting probabilities in a magnetic-breakdown network as a function of field, and its disappearance along the minima in conjunction with the giant magnetoresistance is consistent with the notion of vanishing magnetic breakdown.<sup>15</sup> The magnetoresistance at the angles  $\varphi_n$  is very similar to that of  $\alpha$ - $(BEDT-TTF)_2NH_4Hg(SCN)_4$ , which does not form a DW state, and exhibits metallic, simple closed-orbit behavior with only a single SdH frequency.<sup>19</sup>

The anomalous splitting of the fundamental closed-hole-orbit frequency that appears in the LTS has been the subject of considerable attention.<sup>20,21</sup> In Fig. 3 we show a detailed investigation of the effect for  $\varphi=0$  (central maximum),  $\varphi_1$ , and for the second maximum. Here again we see that phenomena associated with the LTS, in this case the second series oscillation, is virtually gone at the angle  $\varphi_1$ , but reappears at the second maximum. The wave form shown in Fig. 3 indicates that there are two *uncorrelated* contributions to the SdH wave form, one from the metallic FS ( $\alpha$ ), and one

from the reconstructed FS ( $\alpha'$ ). Since the magnetic-breakdown probability  $P_{MB}$  vanishes at  $\varphi_n$ , the orbit  $\alpha'$  (which is identical to  $\alpha$  in frequency) must also disappear since it is a magnetic-breakdown orbit. Figure 3 clearly shows this. This is the strongest evidence for the physical separation (separate domains) of metallic and density-wave phases in the material: such a morphology is a necessary condition for the uncorrelated addition of  $\alpha$  and  $\alpha'$ . The relative position in field of the peaks in  $\alpha$  and  $\alpha'$  may correspond to the relative position in energy of the Landau levels and the Fermi levels, which may be slightly different in the metallic and DW phases.

There are further implications and consequences of our domain model, one of which is given in Fig. 4. Here we show very low-temperature magnetoresistance measurements on a  $M=TI$  sample at  $\varphi_1$  and  $\varphi_2$ , where a very low-frequency oscillation is apparent. This oscillation has a very small SdH frequency of order 10 T, and is only observed at low fields<sup>22</sup> where the magnetic-breakdown probability is small. It corresponds to an orbit with a very small extremal cross section and is most likely the result of the overlap of three closed Q2D orbits in the reconstructed FS (see Fig. 4 inset). For  $\varphi=0$  this orbit is never observed at such high fields since  $P_{MB}$  is large and  $\alpha'$  is the dominant contribution from the reconstructed FS. However, for  $\varphi_n$ , where  $P_{MB}$  vanishes, this orbit is the only allowed contribution from the reconstructed FS.

Our model reconciles otherwise contradictory observations that have arisen in the literature. The  $\beta$  orbit, which involves 100% of the metallic BZ cannot be obtained from the reconstructed FS topology. However, if both phases coexist, then orbits from the reconstructed FS and the  $\beta$  orbit can both be observed. There have also been widely differing reports in the literature on the details of magnetotransport and observed SdH oscillation frequencies and their corresponding oscillation amplitudes.<sup>5,23</sup> The relative concentration of metallic and density-wave domains in any one sample in the LTS should depend on extrinsic parameters such as quality, shape, cooling rate, strain (from leads or mounting), etc. Generally, adverse conditions should reduce the concentration of domains in the DW phase, since it is probably more susceptible. In cases where one domain type dominates, the behavior will be predominantly metallic or DW.

The hysteretic behavior at the kink field is indicative of a first-order phase transition akin to the effect of a magnetic field on a superconductor, and suggests a similar formation of coexisting states. Passage above the kink field returns the entire sample to the metallic state as indicated by the disappearance of the LTS magnetotransport properties. As the field is lowered, DW domains begin to re-form, with different concentrations dependent on the sample history and surrounding environment.

There appears to be approximately equal numbers of metallic and DW domains, indicating that the long-range order of the DW domains is small. We speculate that Coulomb and exchange interaction between the DW and the reconstructed Q2D carriers inhibits long-range coherence.<sup>24</sup> The observation of SdH oscillations defines a lower limit for the domain size given by  $A_r = 2\pi\hbar F/eH^2$ , where  $A_r$  is the real-space area,  $F$  is the SdH frequency, and  $H$  is the applied magnetic field.<sup>16</sup> The DW domains must be at least the size of  $\alpha'$ ,

while the metallic regions must accommodate orbits as large as  $\beta$ . At 10 T this results in areas of  $2.77 \times 10^6$  and  $1.86 \times 10^7 \text{ \AA}^2$ , respectively. The structure of these domains remains to be resolved, and additional experiments are needed.

In summary, we propose that the  $\alpha$ -(BEDT-TTF)<sub>2</sub>M Hg(SCN)<sub>4</sub> materials (excluding  $M = \text{NH}_4$ ) form a mixed state at low temperatures consisting of physically separate metallic and density-wave domains. The model presented here is distinctly different from previous models for the dual-peak SdH oscillations,<sup>20</sup> and for the ADMRO effect.<sup>12</sup> The relative concentration of domains will depend on the sample quality, extrinsic parameters, and history. Hysteresis (first-order behavior) associated with crossing the kink field is a

result of the destruction (upsweep) and reestablishment (downsweep) of the DW domains. Our angular-dependent experimental results strongly suggest that at the special angles  $\varphi_n$ , the magnetic-breakdown probability in the DW Fermi surface vanishes. The precise mechanism for this behavior deserves further attention.

Work at Boston University was supported under NSF Grant No. DMR-92-14889. The authors are indebted to the staffs of the FBNML and the NHFML (both supported by the NSF) where these experiments were carried out. The authors wish to thank Dr. T. Ziman for valuable assistance with the Fermi-surface calculations, and Dr. S. Uji for useful discussions.

- <sup>1</sup>H. Mori, S. Tanaka, M. Oshima, G. Saito, T. Mori, M. Maruyama, and H. Inokuchi, *Bull. Chem. Soc. Jpn.* **63**, 2183 (1990).
- <sup>2</sup>T. Sasaki, H. Sato, and N. Toyota, *Synth. Met.* **41-43**, 2211 (1991).
- <sup>3</sup>H. Mori, I. Hirabayashi, S. Tanaka, T. Mori, H. Inokuchi, K. Oshima, and G. Satio, *Synth. Met.* **55-57**, 2443 (1993).
- <sup>4</sup>N. Kinoshita, M. Tokumoto, and H. Anzai, *J. Phys. Soc. Jpn.* **59**, 3410 (1990).
- <sup>5</sup>M. V. Kartsovnik, A. E. Kovalev, and N. D. Kushch, *J. Phys. I France* **3**, 1187 (1993). The exact shape of the Fermi surface reconstruction is highly sensitive to the choice of nesting vector  $Q$ .
- <sup>6</sup>J. S. Brooks, C. C. Agosta, S. J. Klepper, M. Tokumoto, N. Kinoshita, H. Anzai, S. Uji, H. Aoki, A. S. Perel, G. J. Athas, and D. A. Howe, *Phys. Rev. Lett.* **69**, 156 (1992).
- <sup>7</sup>T. Sasaki and N. Toyota, *Solid State Commun.* **82**, 447 (1992).
- <sup>8</sup>M. Tokumoto, A. G. Swanson, J. S. Brooks, C. C. Agosta, S. T. Hannahs, N. Kinoshita, H. Anzai, and J. R. Anderson, *J. Phys. Soc. Jpn.* **59**, 2324 (1990).
- <sup>9</sup>S. Uji, H. Aoki, J. S. Brooks, A. S. Perel, G. J. Athas, S. J. Klepper, C. C. Agosta, and D. A. Howe, *Solid State Commun.* **88**, 683 (1993).
- <sup>10</sup>T. Osada, A. Kawasumi, R. Yagi, S. Kagoshima, N. Miura, M. Oshima, H. Mori, T. Nakamura, and G. Saito, *Solid State Commun.* **75**, 901 (1990).
- <sup>11</sup>T. Sasaki and N. Toyota, *Phys. Rev. B* **49**, 10 120 (1994).
- <sup>12</sup>Y. Iye, R. Yagi, N. Hanasaki, S. Kagoshima, H. Mori, H. Fujimoto, and G. Saito, *J. Phys. Soc. Jpn.* **63**, 674 (1994).
- <sup>13</sup>J. Caulfield, J. Singleton, P. T. J. Henriks, J. A. A. J. Perenboom, F. L. Pratt, M. Doportto, W. Hayes, M. Kurmoo, and P. Day, *J. Phys. Condens. Matter* **6**, L155 (1994).
- <sup>14</sup>A. E. Kovalev, M. V. Kartsovnik, R. P. Shibaeva, L. P. Rozenberg, and I. F. Schegolov, *Solid State Commun.* **89**, 575 (1994).
- <sup>15</sup>The dynamics of the related magnetic-breakdown network in magnesium are formulated by L. M. Falicov, A. B. Pippard, and P. R. Sievert, *Phys. Rev.* **151**, 498 (1966).
- <sup>16</sup>D. Shoenberg, *Magnetic Oscillations in Metals* (Cambridge University Press, Cambridge, England, 1984).
- <sup>17</sup>A. B. Pippard, *Magnetoresistance in Metals* (Cambridge University Press, Cambridge, England, 1989).
- <sup>18</sup>We have estimated the gap size to be  $\Delta \approx 10 \text{ K}$  by using Arrhenius analysis [ $\rho/\rho_0 = \exp(-2\Delta/k_b T)$ ] to fit the exponential rise of the central maximum between 4–10 K.
- <sup>19</sup>J. Wosnitzer, G. W. Crabtree, H. H. Wang, U. Geiser, J. M. Williams, and K. D. Carlson, *Phys. Rev. B* **45**, 3018 (1992), and references therein.
- <sup>20</sup>T. Sasaki and N. Toyota, *Phys. Rev. B* **48**, 11 457 (1993).
- <sup>21</sup>S. Uji, H. Aoki, M. Tokumoto, N. Kinoshita, H. Anzai, J. S. Brooks, A. S. Perel, G. J. Athas, S. J. Klepper, C. C. Agosta, and D. A. Howe (unpublished).
- <sup>22</sup>S. Uji, H. Aoki, M. Tokumoto, T. Kinoshita, N. Kinoshita, Y. Tanaka, and H. Anzai, *Phys. Rev. B* **49**, 732 (1994).
- <sup>23</sup>F. L. Pratt, J. Singleton, M. Doportto, A. J. Fisher, T. J. B. M. Janssen, J. A. A. J. Perenboom, M. Kurmoo, W. Hayes, and P. Day, *Phys. Rev. B* **45**, 13 904 (1992).
- <sup>24</sup>*Charge Density Waves in Solids*, edited by L. P. Gor'kov and G. Grüner (Elsevier, New York, 1989).

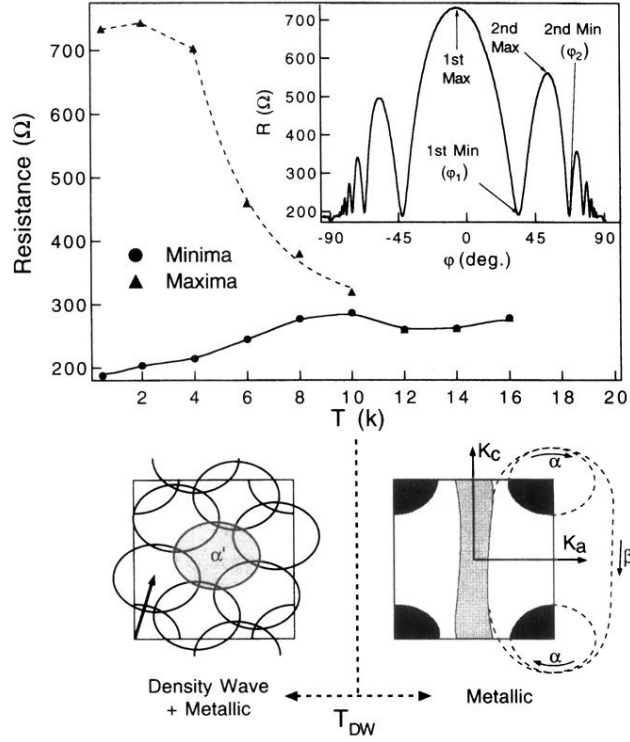


FIG. 1. Temperature dependence of the ADMRO extrema above and below the LTS phase transition ( $T_{DW}=10$  K) for  $M=Rb$  at  $H=14$  T. The inset shows ADMRO at  $T=0.5$  K with arrows indicating the extremal points relevant to this paper. Arrhenius analysis of the maximum between  $4 < T < 10$  results in a  $\Delta \approx 10$  K gap. The calculated metallic state FS, and the proposed coexistence of the metallic and reconstructed density-wave FS are shown separated by the LTS phase boundary. Magnetic-breakdown trajectories and the DW nesting vector  $Q$  (arrow) are highlighted.

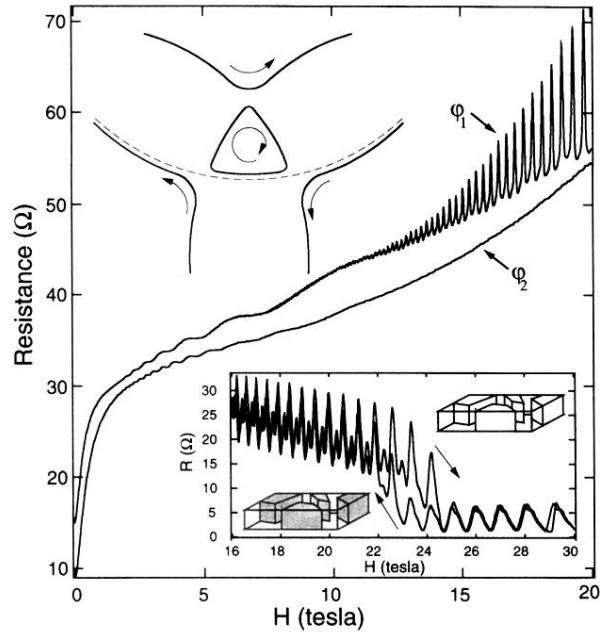


FIG. 4. Full field sweep of  $M=TI$  at 100 mK along  $\varphi_1$  and  $\varphi_2$ . Slow SdH oscillations appear at both these angles corresponding to a zero-angle area of  $\sim 10$  T (SdH oscillations corresponding to  $\alpha$  are suppressed at the large-angle  $\varphi_2$ ). The upper-left inset identifies the origin of this oscillation at the small triangular-hole orbit at the MB junctions. The solid lines represent Bragg-scattered paths, while the dashed line is the high-field magnetic-breakdown limit. The kink field hysteresis for  $M=K$  is shown in the lower-right inset. Below  $H_k$ , domains of reconstructed density-wave (shaded) and normal metallic (clear) regions coexist, while above the kink, all regions are normal metallic.